American Mineralogist, Volume 104, pages 1469–1480, 2019

Gasparite-(La), $La(AsO_4)$, a new mineral from Mn ores of the Ushkatyn-III deposit, Central Kazakhstan, and metamorphic rocks of the Wanni glacier, Switzerland

Oleg S. Vereshchagin[1,*], Sergey N. Britvin[1,6], Elena N. Perova[1], Aleksey I. Brusnitsyn[1], Yury S. Polekhovsky[1], Vladimir V. Shilovskikh[2,3], Vladimir N. Bocharov[2], Ate van der Burgt[4], Stéphane Cuchet[5], and Nicolas Meisser[6]

[1]Institute of Earth Sciences, St. Petersburg State University, University Emb. 7/9, 199034 St. Petersburg, Russia. Orcid 0000-0002-4811-2269
[2]Geomodel Centre, St. Petersburg State University, Uliyanovskaya St. 1, 198504 St. Petersburg, Russia
[3]Institute of Mineralogy, Urals Branch of the Russian Academy of Sciences, Miass 456317, Russia
[4]Geertjesweg 39, NL-6706EB Wageningen, The Netherlands
[5]ch. des Bruyeres 14, CH-1007 Lausanne, Switzerland
[6]Musée cantonal de géologie, Université de Lausanne, Anthropole, 1015 Lausanne, Switzerland
[7]Kola Science Center, Russian Academy of Sciences, Fersman Str. 14, 184209 Apatity, Murmansk Region, Russia

Abstract

Gasparite-(La), $La(AsO_4)$, is a new mineral (IMA 2018-079) from Mn ores of the Ushkatyn-III deposit, Central Kazakhstan (type locality) and from alpine fissures in metamorphic rocks of the Wanni glacier, Binn Valley, Switzerland (co-type locality). Gasparite-(La) is named for its dominant lanthanide, according to current nomenclature of rare-earth minerals. The occurrences and parageneses in both localities are distinct: minute isometric grains up to 15 μm in size, associated with friedelite, jacobsite, pennantite, manganhumite series minerals (alleghanyite, sonolite), sarkinite, tilasite, and retzian-(La) are typically embedded into calcite-rhodochrosite veinlets (Ushkatyn-III deposit) vs. elongated crystals up to 2 mm in size in classical alpine fissures in two-mica gneiss without indicative associated minerals (Wanni glacier). Their chemical compositions have been studied by EDX and WDX; crystal-chemical formulas of gasparite-(La) from the Ushkatyn-III deposit (holotype specimen) and Wanni glacier (co-type specimen) are $(La_{0.65}Ce_{0.17}Nd_{0.07}Ca_{0.06}Mn_{0.05}Pr_{0.02})_{1.02}[(As_{0.70}V_{0.28}P_{0.02})_{1.00}O_4]$ and $(La_{0.59}Ce_{0.37}Nd_{0.02}Ca_{0.02}Th_{0.01})_{1.01}[(As_{0.81}P_{0.16}Si_{0.02}S_{0.02})_{1.01}O_4]$, respectively. In polished sections, crystals are yellow and translucent with bright submetallic luster. Selected reflectance values R_1/R_2 (λ, nm) for the holotype specimen in air are: 11.19/9.05 (400), 11.45/9.44 (500), 10.85/8.81 (600), 11.23/9.08 (700). The structural characteristics of gasparite-(La) were studied by means of EBSD (holotype specimen), XRD, and SREF (co-type specimen). Gasparite-(La) has a monoclinic structure with the space group $P2_1/n$. Our studies revealed that gasparite-(La) from the Ushkatyn-III deposit and Wanni glacier have different origins. La/Ce and As/P/V ratios in gasparite-(La) may be used as an indicator of formation conditions.

Keywords: Gasparite-(La), new mineral, arsenate, REE, Mn ores, monazite-type structure, Ushkatyn-III, Kazakhstan, Wanni glacier, Binn Valley, Switzerland

Introduction

In the course of this study, we described a new rare-earth element (REE) arsenate mineral gasparite-(La) [$La(AsO_4)$, IMA 2018-079] from the Ushkatyn-III deposit, Central Kazakhstan, and the Wanni glacier, Binn Valley, Switzerland. Gasparite-(La) is named for the dominant lanthanide according to current nomenclature of REE minerals (Bayliss and Levinson 1988).

The type locality of gasparite-(La) is the Ushkatyn-III deposit, Central Kazakhstan. Minute isometric grains of gasparite-(La) up to 15 μm in size were discovered in samples from the Ushkatyn-III deposit collected during field work in 2017. The holotype specimen of gasparite-(La) was deposited at the Mineralogical Museum of St. Petersburg State University, St. Petersburg, Russia, catalog number 19692.

The co-type locality of gasparite-(La) is the Wanni glacier, Binn Valley, Valais, Switzerland. Elongated crystals of gasparite-(La) up to 2 mm in size were discovered in autumn 2005 and visually classified as "monazite." Because of their unusual appearance, the material was subjected to further analyses, and recognized as likely identical to the gasparite-(La) later discovered in the Ushkatyn-III deposit. The co-type specimen from Wanni glacier is preserved in Musée Cantonal de Géologie in Lausanne under catalog number MGL 093518.

The use of crystals from different localities allowed us to describe the whole range of physical and chemical properties of gasparite-(La), investigate its crystal chemistry and identify some features characteristic of different genetic types of deposits.

REE-arsenates are among rare minerals: CNMNC IMA has approved only 14 mineral species to date. Most of them

* E-mail: o.vereshchagin@spbu.ru

0003-004X/19/0010–1469$05.00/DOI: https://doi.org/10.2138/am-2019-7028

are representative of Ce-dominant species, and only three La-dominant minerals have been discovered (Modresky 1983; Dunn et al. 1984; Mills et al. 2010).

Despite the limited number of approved mineral species, REE-arsenates are widely distributed in distinct mineral assemblages at numerous localities. Mineralogical information about arsenates (both discovered and crystal-chemically characterized) provides a key to understanding the occurrence and subsequent evolution of many localities (e.g., Campbell and Nordstrom 2014; Majzlan et al. 2014; Wu et al. 2018; Yang et al. 2018).

REE-arsenates have been reported from several postmagmatic and metasedimentary rocks, whose mineral compositions were strongly influenced by late hydrothermal fluids (metasomatic replacement). In the Slovak rhyolites (Ondrejka et al. 2007), primary monazite-(Ce) and xenotime-(Y) were transformed into secondary gasparite-(Ce) and chernovite-(Y), respectively. In case of the granite cupola at Zinnwald (Germany) or Cínovec (Czech Republic), As-rich hydrothermal fluids dissolved and severely altered primary magmatic REE–Y–Th–U–Zr mineralization and gave rise to the formation of REE-arsenates: arsenoflorencite-(Ce), chernovite-(Y), and hydrous xenotime-(Y)-chernovite-(Y) solid solutions (Förster et al. 2011). In the Hora Svaté Kateøiny granite (Czech Republic), reaction with oxidizing As-bearing fluids caused the decomposition of xenotime-(Y), and led to the precipitation of chernovite-(Y) and the incorporation of As into altered zircon and thorite (Breiter et al. 2009). Migrating As-bearing solutions are also believed to have formed the remarkable, classical assemblage of numerous arsenates and arsenites in the Wanni glacier/Mt. Cervandone area at the frontier between the Binn Valley (Switzerland) and Alpe Devero (Italy) (Graeser and Roggiani 1976; Hofmann and Knill 1996; Guastoni et al. 2006). Besides indirect evidence of the presence of multiple REE-arsenates in close association, several minerals show direct evidence of originating from such fluids: gasparite-(Ce) was found as a reaction rim around synchysite-(Ce) (Graeser and Schwander 1987), deveroite-(Ce) was found as a dissolution product of cervandonite-(Ce) (Guastoni et al. 2013), agardite-(Y) (Gatta et al. 2018), and rhabdophane-(Ce) on synchysite-(Ce) (Cuchet et al. 2019), and uranyl arsenates on cafarsite (Appiani et al. 2017).

Manganese rocks of different geneses are often enriched in arsenic, reaching concentrations several times higher than the mean values for both sedimentary rocks and for the upper part of the continental crust as a whole (Li and Schoonmaker 2003; Maynard 2003). More than half of all discovered Mn-arsenates were found in the famous Mn deposits in Franklin/Sterling Hill, U.S.A.; Långban, Sweden, and Moss Mine, Sweden.

Both Långban, Sweden, and Franklin/Sterling Hill, New Jersey, are represented by strongly metamorphosed Precambrian rocks of sedimentary origin (Frondel and Baum 1974; Holtstam and Langhof 1999; Lundström 1999). According to Frondel and Baum (1974), the only primary As-bearing ore minerals in Franklin/Sterling Hill are löllingite, arsenopyrite, and the calcium arsenate svabite. In both cases (Långban and Franklin/Sterling Hill), the greatest mineralogical diversity is found among the minerals in veins and fissures.

A limited number of small Fe–Mn–(Ba,V,As,Sb,Be,W,REE) deposits, containing arsenates including REE-arsenates, have been found in the Swiss, Italian, and Austrian Alps (Abrecht 1990; Brugger and Giere 1999; Cabella et al. 1999; Brugger and Meisser 2006). These occurrences are thought to represent syngenetic exhalative Fe-Mn accumulations (Majzlan et al. 2014) metamorphosed during the Alpine orogeny (Abrecht 1990; Brugger and Meisser 2006). Brugger and Meisser (2006) argued that the chemical composition of the rocks reflects the pre-metamorphic state. Cabella et al. (1999) reported that the abundance of arsenates reduces sharply as a function of proximity to the Fe-Mn ores. The same genetic conclusion was made for Mn-rich metamorphic rocks in the Hoskins manganese mine, New South Wales, Australia (Ashley 1989).

Gasparite-(Ce) is, although generally rare, the most widely distributed REE-arsenate. The type locality for gasparite-(Ce), and several other REE-arsenates and arsenites, is Mt. Cervandone, a summit on the frontier of Italy (Cervandone, Val Devero) and Switzerland (Wanni glacier, Binntal), where it occurs in metasedimentary rocks (Graeser and Schwander 1987). Besides that, gasparite-(Ce) was found as an accessory mineral in the Black Range Tin District, New Mexico, U.S.A. (Foord et al. 1991, 1999); Tisovec-Rejkovo, Slovakia (Ondrejka et al. 2007); Beryllium Virgin Claim, New Mexico, U.S.A. (Anthony et al. 2000); Chudnoe and Nesterovskoe occurrences, Maldynyrd Range, Prepolar Ural, Russia (Moralev et al. 2005); Kesebol deposit, Sweden (Kolitsch and Holtstam 2004; Kolitsch et al. 2004); Grubependity Lake cirque, Maldynyrd Range, Prepolar Ural, Russia (Mills et al. 2010); Artana, Carrara, Apuane Alps, Italy (Mancini 2000); Tanatz Alp, Switzerland (Roth and Meisser 2013), and Ponte dei Gonazzi, the Maritime Alps, Italy (Cabella et al. 1999).

In most cases, lanthanum is present in gasparite in subordinate amounts (<15 wt% La_2O_3). However, La-dominant grains of gasparite were found in Mn-enriched metamorphosed rocks from the Ponte dei Gonazzi, the Maritime Alps, Italy (up to 45 wt% La_2O_3; Cabella et al. 1999) and in A-type rhyolite from Western Carpathians, Slovakia (up to 26 wt% La_2O_3; Ondrejka et al. 2007). The particle size was insufficient to allow for the investigation of the properties of La-dominant gasparite, and therefore these studies did not describe their findings as a new mineral phase.

Occurrence

Ushkatyn-III deposit, Central Kazakhstan

The Ushkatyn-III deposit (48°16′06″N, 70°10′43″E) is located in Central Kazakhstan 300 km southwest of the city of Karaganda and 20 km to the northeast of the village Zhayrem. The deposit was discovered in 1962. Manganese ore mining started in 1982 and has continued to date. Beginning in 2015, barite-lead ores started to be mined. As of 2015, manganese ore reserves amounted to 102 million tons, with an average Mn content of 24 wt% and Fe 3.5 wt%, and barite-lead ore reserves of 42 million tons, with an average Pb = 2.6 wt% and $BaSO_4$ = 19 wt% [Annual report for the year 2015, Publishing house JSC ZHGOK, 103 p (in Russian).].

The geological structure of the deposit was considered in the works of Kayupova (1974), Buzmakov et al. (1975), Mitryaeva (1979), Rozhnov (1982), and Skripchenko (1980, 1989).

The Ushkatyn-III deposit is located in the western part of the Zhailinsky graben-syncline. This large riftogenic structure originated in the Late Devonian during the destruction of the epi-Caledonian Central-Kazakhstan continental block. The clay-siliceous-carbonate rocks of the Famennian stage of the Upper Devonian are ore-bearing. In the eastern part of the deposit, they are represented by reefogenic limestones containing stratiform barite-lead mineralization. In the western part of the deposit, these rocks are replaced by detrital and nodular-layered siliceous limestones containing layers of manganese ores. Altogether, there are fourteen ore layers, each of which has a well-marked, rhythmically stratified structure with alternating layers of manganese ore and limestones. The thickness of individual rhythms range from 15 cm up to 1 m, and the total thickness of ore layers varies from 5 to 25 m. A series of adjacent layers are grouped into a large pack, traced over a strike of more than 1.5 km, a drop of 760 m, and a thickness of 50–150 m. Volcanic rocks are present on the deposit but in volumetric inferior amount (no more than 10% of the whole volume of the ore-bearing strata).

Manganese ores are fine-grained rocks (average size of mineral grains 10–30 μm) with layered and lenticular-banded textures. Altogether, more than 60 minerals have been identified in manganese ores of the Ushkatyn-III deposit by optical, electron microscopy, powder X-ray diffraction, and electron microprobe analysis (Kayupova 1974; Brusnitsyn et al. 2017, 2018). The main minerals are braunite, hausmannite, quartz, calcite, rhodochrosite, tephroite, friedelite, and minerals of manganhumite series (sonolite, alleghanyite). The most characteristic secondary minerals are hematite, jacobsite, rhodonite, caryopilite, pennantite, manganese clinochlore, albite, and barite. Among the most interesting accessory minerals are cinnabar, pyrobelonite, cerianite-(Ce), fluorite, and several REE and arsenate minerals: sarkinite, svabite, tilasite, and retzian group minerals.

Manganese ores can be divided into two types: (1) braunite: braunite + calcite + quartz ± albite, and (2) hausmannite: hausmannite + calcite + rhodochrosite ± tephroite (sonolite, alleghanyite) ± friedelite (caryopilite). These types of ores can form separate layers and can be combined within a single layer. In the latter case, the mineral composition of ores changes as a result of the substitution of braunite for hausmannite/associated silicates/rhodochrosite.

The first arsenates in the Ushkatyn-III deposit were discovered in the early 1970s (Kayupova 1974). However, due to the lack of appropriate analytical instruments, only relatively big grains of minerals (sarkinite, tilasite, and brandtite) were identified.

Gasparite-(La) was found in hausmannite ores, associated with other arsenates. The mineral was found in microveins cutting layers of hausmannite, calcite, and rhodochrosite. Gasparite-(La) is associated with friedelite, jacobsite, pennantite, manganhumite series minerals (alleghanyite, sonolite), sarkinite, tilasite, and retzian-(La). The microveins containing gasparite-(La) range in size from micrometers to 1–5 mm in thickness and to 1–3 cm in length. Gasparite-(La) forms grains of 2–25 μm in size, as well as aggregates with other arsenates of irregular shape up to 50 μm and was found in association with retzian-(La) and alleghanyite (Fig. 1a).

Wanni glacier, Binn Valley, Valais, Switzerland

The Wanni glacier, located in the Binn Valley, Valais (Wallis), Switzerland, represents the Swiss side of the Scherbadung or Pizzo Cervandone of which the Italian side is located in Alpe Devero, Piemonte, Italy. Its mineral assemblage extends to both sides of this mountain and is the type locality of seven REE-arsenates and REE-arsenites (Graeser 1966; Graeser and Schwander 1987; Armbruster et al. 1988; Demartin et al. 1994; Graeser et al. 1994; Guastoni et al. 2006, 2013) and its geology has been summarized in Streckeisen et al. (1974), Steck (1987), Klemm et al. (2004), Hettman et al. (2014), and Bergomi et al. (2017). The REE-As mineralization is hosted in two-mica gneisses of the Monte Leone nappe and extends multiple kilometers westward to the Gischi glacier (Graeser and Roggiani 1976), Chummibort (Cuchet et al. 2005), and Mättital (Krzemnicki 1992, 1997) and eastward to the Lercheltini area. According to Krzemnicki and Reusser (1998), several Pre-alpine ore concentrations within this nappe were locally re-mobilized during Alpine metamorphism, thus generating some unique hydrothermal mineralization.

The sample containing gasparite-(La) was found in rocks

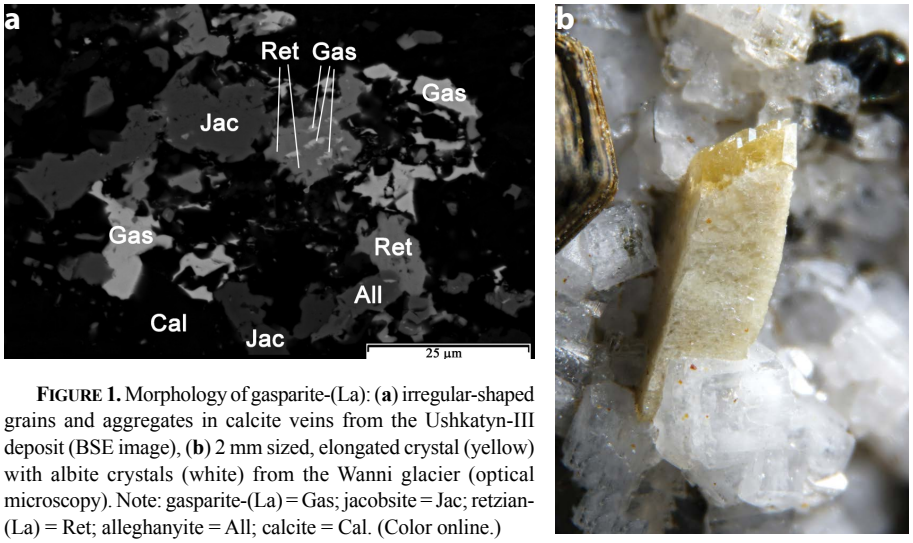

FIGURE 1. Morphology of gasparite-(La): (**a**) irregular-shaped grains and aggregates in calcite veins from the Ushkatyn-III deposit (BSE image), (**b**) 2 mm sized, elongated crystal (yellow) with albite crystals (white) from the Wanni glacier (optical microscopy). Note: gasparite-(La) = Gas; jacobsite = Jac; retzian-(La) = Ret; alleghanyite = All; calcite = Cal. (Color online.)

of the Monte Leone nappe (46°19′20,N, 8°12′48E). The Monte Leone nappe includes fine-grained banded orthogneisses and minor coarse-grained augen gneiss interlayered with paragneisses, hornblende gneisses, and amphibolites (Klemm et al. 2004; Hettmann et al. 2014) and shows a penetrative amphibolite-facies metamorphic overprint of Alpine age (Maxelon and Mancktelow 2005; Bergomi et al. 2017).

The specimen containing gasparite-(La) was extracted from a small, classical Alpine fissure. The stratum containing the fissure with gasparite-(La) is a fine-layered, two-mica gneiss and is located outside the main Cu-As-F-mineralization that has cafarsite as the dominating As-containing mineral. Based on our observation, the As-enrichment is not very dense in this sublayer. While the occurrence of REE-arsenates [chernovite-(Y), gasparite-(Ce)] is increased, arsenites (cafarsite and asbecasite) are a diminished.

The specimen containing gasparite-(La) (containing three elongated crystals) was located on one side of the cavity; the remainder was empty, apart from minerals that belong to the classical fissure parageneses: minor titanite, quartz, feldspar, and albite. Crystals of gasparite-(La) are prismatic of a size up to 2 mm (Fig. 1b). An interesting feature of the studied crystals is that their prism appears non-translucent (as if fractured) and yellow, whereas the summit faces are perfectly, gemmy translucent and more orange.

Elemental composition

Elemental compositions of rock-forming minerals were studied on the carbon-coated polished sections using a Hitachi S-3400N scanning electron microscope equipped with an Oxford X-Max 20 energy-dispersive X-ray spectrometer (EDX). EDX spectra were obtained under the following conditions: 20 kV accelerating voltage and 2 nA beam current with an acquisition time of 30 s per spectrum.

Elemental analyses for gasparite-(La) were obtained using an Inca Wave 500 wavelength-dispersive X-ray (WDX) spectrometer also equipped on the microscope mentioned above. WDX spectra collection conditions were: 20 kV, 10 nA, beam diameter 5 μm, 30 s peak, and 30 s background collection per element, XPP matrix correction. Fe metal, Mn metal, V metal, InP, InAs, wollastonite, Th-, Y-, La-, Ce-, Nd-, and Sm-bearing glass standard samples (MAC-standards) were used for spectrometer calibration.

Preliminary EDX analyses showed that gasparite-(La) from the Ushkatyn-III deposit has almost no chemical zoning or consistent element ratios; all analyzed grains showed La > Ce > Nd and As > V > P. In the case of gasparite from the Ushkatyn-III deposit, Central Kazakhstan, five analyses (WDX) from three different grains were performed on one carbon-coated polished section (Table 1). The empirical formula of gasparite-(La) from the Ushkatyn-III deposit, based on four oxygen atoms, is $(La_{0.65}Ce_{0.17}Nd_{0.07}Ca_{0.06}Mn_{0.05}Pr_{0.02})_{1.02}[(As_{0.70}V_{0.28}P_{0.02})_{1.00}O_4]$.

One elongated crystal of gasparite from Wanni glacier was studied by EDX and WDX analyses. EDX analysis showed that the crystal has chemical zoning: its La/Ce/Nd ratio varies significantly, whereas As/P ratio is approximately constant (Fig. 2). The optically more translucent summit of the crystal is La-dominant, while the prismatic part of the crystal is Ce-dominant; and thus, it represents gasparite-(Ce). We performed five WDX analyses from the summit of the crystal and the overall empirical formula of gasparite-(La) from the Wanni glacier, based on four oxygen atoms, is $(La_{0.59}Ce_{0.37}Nd_{0.02}Ca_{0.02}Th_{0.01})_{1.01}[(As_{0.81}P_{0.16}Si_{0.02}S_{0.02})_{1.01}O_4]$. The simplified formula of gasparite-(La) from both the Ushkatyn-III deposit and the Wanni glacier is $La(AsO_4)$.

Table 1. Chemical composition of gasparite-(La)

Constituent	Ushkatyn-III deposit		Wanni glacier	
	wt%	Range	wt%	Range
Fe_2O_3	0.05	0.00–0.16	0.00	0.00
MnO	1.30	0.91–1.96	0.00	0.00
CaO	1.33	0.97–1.54	0.34	0.24–0.48
ThO_2	0.00	0.00	0.58	0.37–0.72
Y_2O_3	0.01	0.00–0.05	0.01	0.00–0.03
La_2O_3	40.21	37.83–41.17	35.59	34.57–36.74
Ce_2O_3	10.69	9.76–11.61	22.55	21.26–23.67
Pr_2O_3	1.46	0.00–1.99	0.29	0.00–0.88
Nd_2O_3	4.24	3.53–4.69	1.04	0.50–1.30
Sm_2O_3	0.09	0.00–0.33	0.07	0.00–0.35
V_2O_5	9.77	8.58–11.21	0.00	0.00
P_2O_5	0.64	0.22–0.99	4.29	4.18–4.45
As_2O_5	30.32	29.46–31.41	34.48	33.27–35.22
Total	100.11		99.24	

Gasparite-(La) belongs to the monazite group, which contain seven monoclinic phosphate and arsenate minerals (Table 2). It is a La-dominant analog of gasparite-(Ce) (Graeser and Schwander 1987) and an arsenate-dominant analog of monazite-(La). According to the Nickel-Strunz Classification, gasparite-(La) belongs to 8.AD (8 = phosphates, arsenates, vanadates; A = phosphates, etc. without additional anions, without H_2O; D = with only large cations).

Physical properties and optical data

Gasparite-(La) crystals are yellow and translucent with bright submetallic luster. The Vickers Hardness Number (VHN) measured on gasparite-(La) from the Wanni glacier was 325 with a range 308–340 kg mm^{-2} (load 20 g) by means of HMV-2T (Shimadzu). This data are in a good agreement with the data on

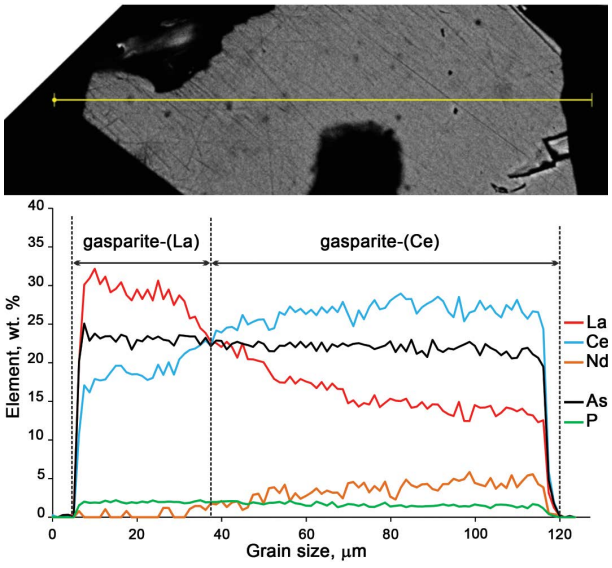

Figure 2. Chemical zoning of a gasparite crystal from the Wanni glacier. (Color online.)

TABLE 2. Comparative crystallographic data for monazite group minerals

Mineral	Gasparite-(La)	Gasparite-(Ce)	Rooseveltite	Monazite-(La)	Monazite-(Ce)	Monazite-(Nd)	Monazite-(Sm)	Cheralite
Chemical formula	$La(AsO_4)$	$Ce(AsO_4)$	$Bi(AsO_4)$	$La(PO_4)$	$Ce(PO_4)$	$Nd(PO_4)$	$Sm(PO_4)$	$CaTh(PO_4)_2$
Crystal system				Monoclinic				
Space group				$P2_1/n$				
a (Å)	6.9576(4)	6.929(3)	6.879(1)	6.8313(10)	6.7880(10)	6.7352(10)	6.6818(12)	6.7085(8)
b (Å)	7.1668(4)	7.129(3)	7.159(1)	7.0705(9)	7.0163(9)	6.9500(9)	6.8877(9)	6.4152(6)
c (Å)	6.7155(4)	6.697(3)	6.732(1)	6.5034(9)	6.4650(7)	6.4049(8)	6.3653(9)	6.4152(6)
β (°)	104.414(1)	104.46(3)	104.84(1)	103.27(1)	103.43(1)	103.68(1)	103.86(1)	103.71(1)
Z				4				
Reference	[a]	[b]	[c]	[d]	[d]	[d]	[d]	[e]

Notes: For comparison u.c.p. given as a>c. [a] This study, Wanni glacier. [b] Kolitsch et al. 2004. [c] Bedlivy and Mereiter 1982. [d] Ni et al. 1995. [e] Raison et al. 2008.

gasparite-(Ce) (VHN = 327 kg mm^{-2}; Graeser and Schwander 1987). Mohs hardness could not be determined because of the tiny sizes of the crystals. The Mohs hardness calculated from the VHN value was approximately 4½.

As gasparite-(La) from the Ushkatyn-III deposit had no chemical zoning, one of its grains was chosen for optical study. In polished sections, gasparite-(La) from the Ushkatyn-III deposit looked dark gray under reflected light. The mineral was slightly anisotropic with $\Delta R_{589} = 2.04\%$. The reflectivity of gasparite-(La) in the air (Supplemental[1] Table S1) was measured against a SiC standard (reflection standard = 474251, no. 545) using MSF-21 spectrophotometer with a monochromator slit of 0.4 mm and a 100 µm zone diameter. The measurement parameters were as follows: lens magnification 21×, aperture 0.4, and $\Delta\lambda$ = 10 nm, SiC. The reflectivity spectrum is shown in Figure 3.

Raman spectra

Gasparite-(La) crystals from both localities were used for Raman studies. Raman spectra (Fig. 4) were recorded with a Horiba Jobin-Yvon LabRAM HR800 spectrometer equipped with an Olympus microscope having 50× and 100× objectives. Raman spectra were excited by an Ar ion laser at a wavelength of 514 nm and a maximum power of 50 mW. The spectra were obtained in the range of 100–4000 cm^{-1} at a resolution of 2 cm^{-1} at room temperature. To improve the signal-to-noise ratio, the number of acquisitions was set to 20. The spectra were processed using licensed Labspec and Origin software. Band fitting was done using a Lorentz function with the minimum number of component bands used for the fitting process (Table 3).

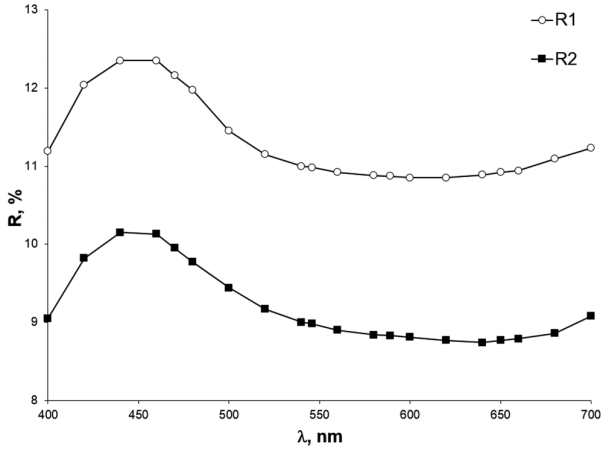

FIGURE 3. Reflectance spectra in the air for gasparite-(La) from the Ushkatyn-III deposit.

Raman spectra of gasparite-(La) from both the Ushkatyn-III deposit and the Wanni glacier were very close to that of synthetic $La(AsO_4)$ (Fig. 4, Table 3). Bands in the region from 4000 to 1100 cm^{-1} were not registered, which means that gasparite-(La) contained no $(OH)^-$ groups. Bands assigned to stretching vibrations ν_1 and ν_3 of arsenate ion are observed in the region 900–800 cm^{-1}. There were bending vibrations ν_2 and ν_4 of arsenate ion in the region of 500–350 cm^{-1}. The lattice vibrations were located below 320 cm^{-1}. The main differences of Raman spectra of the minerals in comparison with the pure synthetic phase were associated with impurities of $(VO_4)^{3-}$ (Ushkatyn-III) and $(PO_4)^{3-}$ (Wanni glacier). Vibrations $\nu_1(PO_4)$ was about 960 cm^{-1}, $\nu_1(VO_4)$ near 840 cm^{-1} (Solecka et al. 2018; Song et al. 2018). In the region of the ν_4 band, the main differences are associated with the overlapping of bands related to $(AsO_4)^{3-}$, $(PO_4)^{3-}$, and $(VO_4)^{3-}$. Raman spectra reveal the predominance of La+Ce in the mineral composition of $\nu_1(AsO_4)$ of 861–863 cm^{-1}. The Raman spectrum of $Ho(AsO_4)$ $\nu_1(AsO_4)$ was about 895 cm^{-1} (Barros et al. 2009). Impurity tetrahedral cations (P,V) did not influence the $\nu_1(AsO_4)$ band shift.

Crystallography

Because gasparite-(La) from the Ushkatyn-III deposit occurs as microscopic grains up to 15 µm in size (Fig. 2) it was not pos-

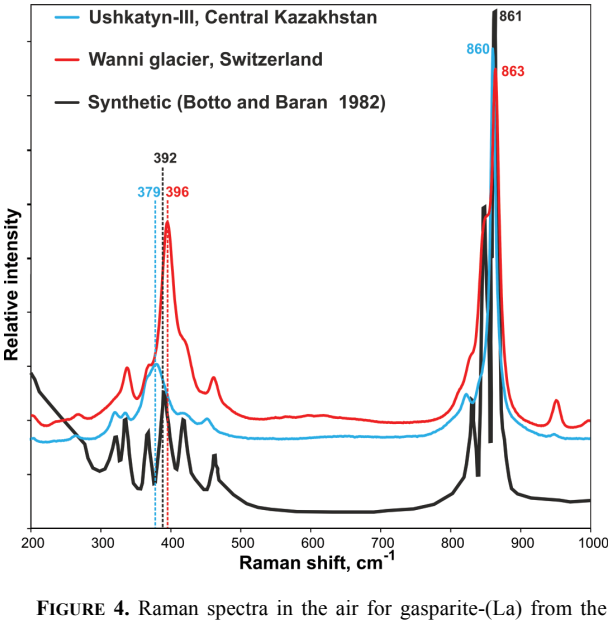

FIGURE 4. Raman spectra in the air for gasparite-(La) from the Ushkatyn-III deposit, gasparite-(La) from the Wanni glacier and synthetic $La(AsO_4)$ (Botto and Baran 1982). (Color online.)

Table 3. Raman spectral signatures of gasparite-(La)

Raman shift, cm^{-1}/Relative Intensity			Assignment	Raman shift (cm^{-1})/Relative Intensity			Assignment
Ushkatyn-III	Wanni glacier	Botto and Baran 1982		Ushkatyn-III	Wanni glacier	Botto and Baran 1982	
92/vw	94/vw			364/vw	367/w	350/vw 367/w	$v_4(AsO_4)$
104/vw	107/w						
126/vw	125/w			379/st	395/st	392/m	$v_2(AsO_4)$
138/vw	139/vw						
153/vw	155/w			422/w	421/m	418/w	$v_4(AsO_4)$
190/vw	190/w						
203/m	203/vw						
				452/w	462/w	440/sh	
						461/w	
			Lattice vibrations				
264/vw	267 vw			822/m	812/sh	798/vw	$v_3(AsO_4)$
320/w		322/w					
334/vw	337/w	336/w					
				843/sh	826/sh	827/m	
					848/sh	845/st	
						872/sh	
				860/vs	864/vs	861/vs	$v_1(AsO_4)$
					951/w		$v_1(PO_4)$

Note: vs = very strong; st = strong; m = medium; w = weak; vw = very weak; sh = shoulder.

sible to determine its crystal structure with single-crystal X-ray diffraction. All diffraction data were obtained by electron backscatter diffraction (EBSD) (Fig. 5). In the case of gasparite-(La) from the Wanni glacier, we managed to isolate the La-enriched zone of the elongated crystal and refine its crystal structure using single-crystal X-ray diffraction. The same crystal fragment was used for powder X-ray diffraction studies.

Powder X-ray diffraction (XRD)

The powder XRD pattern for gasparite-(La) from the Wanni glacier was recorded in Debye–Scherrer geometry using a Rigaku R-AXIS Rapid II diffractometer equipped with a curved (cylindrical) imaging plate detector (r = 127.4 mm). Co$K\alpha$ radiation (λ = 1.79021 Å) was generated by a rotating anode (40 kV, 15 μA) with microfocus tube optics; exposure time was set to 15 min. The data were processed using the osc2xrd program (Britvin et al. 2017) and Stoe WinXPOW software XRD data for gasparite-(La) from the Wanni glacier is presented in Supplemental[1] Table S2 and is similar to that of synthetic $La(AsO_4)$ (Le Berre et al. 2007; JCPDS file 15-0756). Calculated data were obtained using Rietveld analysis of the powder pattern [c = 6.7087(3), b = 7.1499(2), a = 6.9429(2) Å, β = 104.442(2)°].

Single-crystal X-ray diffraction and refinement (SREF)

REE arsenates, chromates, phosphates, and vanadates of $Ln(XO_4)$ type can crystallize in monoclinic (monazite structure) or tetragonal (zircon-type structure) symmetry (Schwarz 1963; Botto and Baran 1982; Clavier et al. 2011). In the REE arsenate and phosphate series, the La, Ce, Pr, and Nd end-members possess the monazite structure (Clavier et al. 2011). REE vanadates have more complex behavior: the majority of REE vanadates (Ce–Lu, Sc) have the zircon-type structure, whereas $La(VO_4)$ crystallizes in both the zircon-type and monazite-type structures (Witzke et al. 2008).

The monazite-type structure was first reported by Mooney (1948) and then refined by several researchers for various REE-phosphates (Feigelson 1964; Ghouse 1968; Beall et al. 1981; Pepin and Vance 1981; Mullica et al. 1984; Mullica et al. 1985; Ni et al. 1995). The structural arrangement in the monazite-type structure

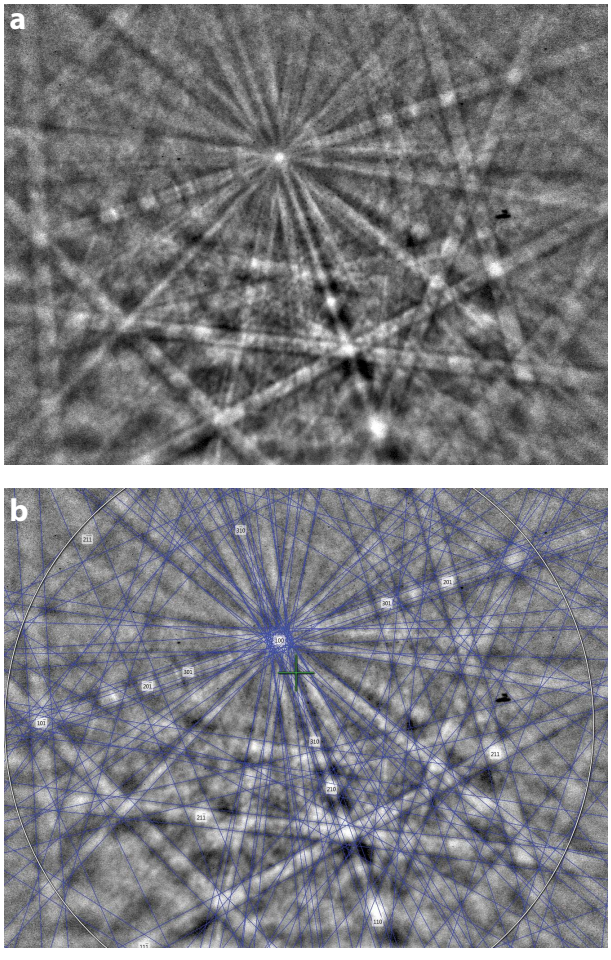

Figure 5. (**a**) EBSD pattern of the gasparite-(La) crystal (30 kV accelerating voltage, 0.3 nA beam current, 5 s exposure per frame, averaging of 20 frames, 1344 × 1024 pixels image size), and (**b**) the pattern indexed with the $P2_1/n$ structure (MAD 0.15, 80 bands are represented on the image). (Color online.)

is based on ninefold coordination of the metallic cation and can be described as an equatorial pentagon interpenetrated by a tetrahedron (Clavier et al. 2011). The tetrahedron located out of the equatorial plane can then be described as a link between the REE O_9 polyhedra, leading to the formation of infinite chains along the c axis.

According to the published data, both synthetic La(AsO_4) (Schmidt et al. 2005) and natural gasparite-(Ce) (Kolitsch et al. 2004) have a monoclinic structure with the space group $P2_1/n$. The crystal structure of gasparite-(La) from the Wanni glacier (co-type specimen) was solved by direct methods and refined to $R_1 = 0.014$ using a SHELX-2015 set of programs (Scheldrick 2015) via Olex2 ver.1.2.8 graphical user interface (Dolomanov et al. 2009) (Tables 4 and 5; Supplemental[1] Table S3). Data collection and structure refinement details are given in Tables 4 and 5 and in the CIF[1] file. The La site is coordinated by nine O atoms, with (La-O) distances of 2.586 (Table 6). The As site was found to be almost fully occupied by As ($As_{0.84}P_{0.16}$), in agreement with the chemical data. The unit-cell parameters of gasparite-(La) are larger than the values for gasparite-(Ce) (Kolitsch et al. 2004), smaller than those for synthetic La(AsO_4) (Schmidt et al. 2005) and in good agreement with the values derived from powder XRD data of the same crystal.

Electron backscatter diffraction (EBSD)

EBSD measurements were performed on an Oxford HKLNordlys Nano EBSD detector equipped on a Hitachi S-3400N scanning electron microscope. Operating conditions are listed in Supplemental[1] Table S4. Both acquisition and analysis of Kikuchi-patterns were made using Oxford AZtecHKL software. Synthetic La(AsO_4) structural data (ICSD) were used as inputs (Schwartz et al. 2009). The sample was polished with progressively smaller polycrystalline diamond suspensions with the ending step of Ar ion etching for 10 min at the final stage (Oxford IonFab 300) to remove amorphized layers for EBSD analysis. The sample was pre-tilted 70° along the normal to the EBSD detector. The fit factor [mean angular deviation (MAD)], which describes the angular deviation between the calculated and measured Kikuchi lines (good fit for deviations <1.0°), is less than 0.3° for synthetic La(AsO_4) and Ce(AsO_4) (Brahim et al. 2002; Kang and Schleid 2005).

Eighteen electron backscatter patterns from three different gasparite-(La) grains were collected (Fig. 6). Good matches were obtained for all patterns using monoclinic La(AsO_4) structure with the space group $P2_1/n$ (Schmidt et al. 2005).

TABLE 4. Crystal data, XRD data collection and structure refinement details for gasparite-(La) from the Wanni glacier

Crystal data	
Chemical formula	$(La_{0.6}Ce_{0.40})[(As_{0.84}P_{0.16})O_4]$
M_r	271.39
Crystal system, space group	Monoclinic, $P2_1/n$
a, b, c (Å)	6.7155(4), 7.1668(4), 6.9576(4)
β (°)	104.414(1)
V (Å^3)	324.32(3)
Z	4
D_x (g/cm^3)	5.558
Crystal size (mm)	0.04 × 0.04 × 0.03
Data collection	
Diffractometer	Bruker APEX-II CCD
Radiation type	MoKα (0.71073 Å)
μ (mm^{-1})	21.95
Absorption correction	Multi-scan
No. of measured, independent and observed [$I > 2s(I)$] reflections	3839, 944, 869
2Θ range for data collection (°)	7.55 to 60.00
Index ranges	$-9 \le h \le 9$, $-9 \le k \le 10$, $-9 \le l \le 9$
Structure refinement	
R_{int}, R_s	0.0207, 0.0175
R_1 [$F^2 > 2\sigma(F^2)$], $wR_2(F^2)$, S	0.014, 0.029, 1.12
No. of reflections	944
No. of parameters	57
$\Delta\rho_{max}$, $\Delta\rho_{min}$ (e/Å^3)	0.76, –0.55

TABLE 5. Fractional atomic coordinates and isotropic displacement parameters (U_{iso}, Å^2) for gasparite-(La) from the Wanni glacier

Site	x	y	z	U_{iso}	Occupancy (<1)
M (4e)	0.40018(2)	0.34494(2)	0.21899(2)	0.00827(6)	$(La_{0.6}Ce_{0.4})$[a]
X (4e)	0.38653(4)	0.16300(4)	0.69644(4)	0.00626(11)	$(As_{0.84}P_{0.16})$
O1 (4e)	0.2803(3)	0.2142(3)	0.8797(3)	0.0131(4)	
O2 (4e)	0.5664(3)	–0.0012(3)	0.7481(3)	0.0133(4)	
O3 (4e)	0.5031(3)	0.3390(3)	0.6113(3)	0.0122(4)	
O4 (4e)	0.1793(3)	0.1075(3)	0.5181(3)	0.0130(4)	

[a] The occupancy of M site was fixed according to electron microprobe data.

DISCUSSION

Crystal chemistry and substitution mechanisms

The REE ratio in gasparite-(La) from the Ushkatyn-III deposit shows no significant variations and in all analyzed grains, La > Ce. The REE ratio in crystals of gasparite-(La) from the Wanni glacier varies significantly from Ce-dominant to La-dominant species in the same crystal (Fig. 2).

Our data revealed a very limited P-for-As substitution (P up to 0.02 apfu) but a large extent of V-for-As substitution (V up to 0.28 apfu) in gasparite-(La) from the Ushkatyn-III deposit (Fig. 7). On the other hand, gasparite-(La) from the Wanni glacier contains no V and exhibits extensive P-for-As substitution (P up to 0.16 apfu).

The impurity of tetrahedral cations (P,V) does not appear to influence the (AsO_4) band shift as isolated tetrahedra [(AsO_4), (PO_4), and (VO_4)] in the gasparite structure surrounded by polyhedral [(LaO_9), (CeO_9), and (NdO_9)]. As a result, cations in the polyhedra have a major impact on the positions of the bands related to As-O vibrations in $(AsO_4)^{3-}$. Both P-for-As and V-for-As are reflected in the appearance of additional bands or broadening of the main bands. The band around 390 cm^{-1} in the case of P-for-As (Wanni glacier), shifts upward, and in the case of V-for-As (Ushkatyn-III deposit), shifts downward (Fig. 4).

No natural vanadates of monazite structure-type have been reported yet. Only wakefieldite group minerals with the zircon structure were reported (Deliens and Piret 1986; Witzke et al. 2008). No experimental evidence for the existence of AsO_4–PO_4 substitution was reported. Cabella et al. (1999) described gasparite-(Ce) enriched with P and V and reported a wide range of V-for-As substitutions (V up to 0.30 apfu) and P-for-As substitutions (P up to 0.15 apfu). Kolitsch et al. (2004) reported that 10% of the As atoms are substituted by P (P up to 0.12 apfu) in gasparite-(Ce).

The crystal chemistry of the MXO_4 monazite-type compounds in general (M = La, Ce; X = As, P, V) have been studied intensively (e.g., Clavier et al. 2011; Kolitsch et al. 2004). Kolitsch et al. (2004) assumed that the substitution of P for As leads to the substantial decrease of the c-parameter, which can be explained by the stacked arrangement along the [001] direction of the XO_4

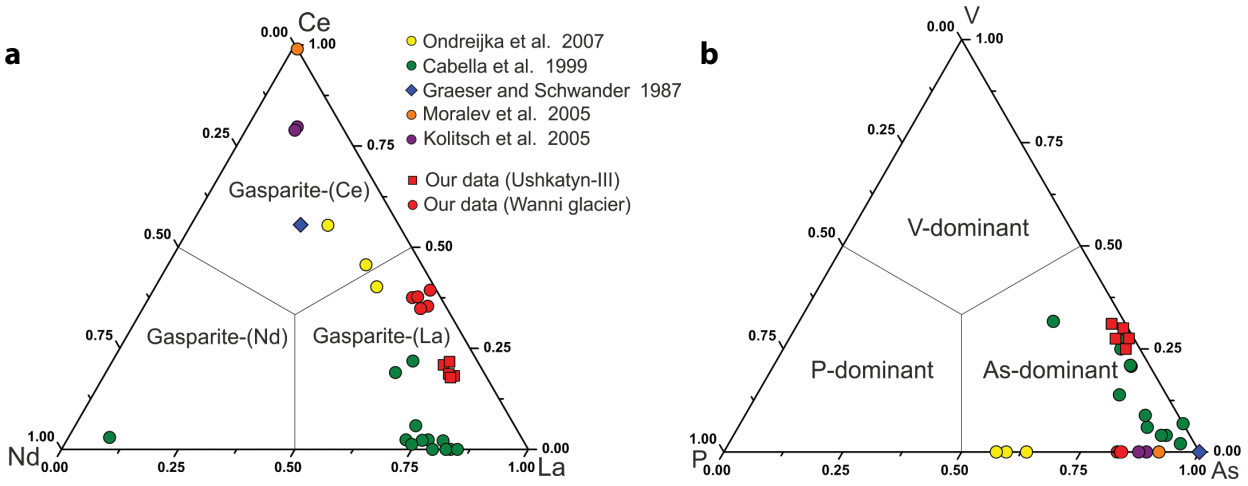

FIGURE 6. Chemical composition variations in gasparite group minerals: (**a**) La-Ce-Nd ratio and (**b**) As-V-P ratio. (Color online.)

groups in the structure.

Our data confirmed that both cell parameters *a* and *c* are influenced mainly by the size of XO_4 tetrahedra (r = 0.99, r = 0.92, respectively; Fig. 8a), whereas the *b* parameter is mainly influenced by the size of the MO_9 polyhedra (r = 0.92; Fig. 8b).

Comparison of $LaXO_4$ monazite-type compounds shows that the (La-O) distance in MXO_4 monazite-type compounds varies significantly: 2.579 [$La(PO_4)$; Ni et al. 1995] to 2.599 Å [$La(AsO_4)$; Schmidt et al. 2005]. This may explain the distortion of LaO_9 polyhedra, which is well correlated to (*X*-O) distance (r = 0.99; Table 6) and could be the reason for the *b* vs. (*M*-O) correlation.

Origin of gasparite-(La)

As stated above, gasparite-(La) was found in occurrence with distinct geological situations. Gasparite-(La) from the Wanni glacier, Binn Valley was found in an alpine fissure with evidence of hydrothermal alteration (well-shaped crystals in an almost empty cavity), whereas gasparite-(La) from the Ushkatyn-III deposit was found in primary Mn ores (irregular-shaped grains in calcite-rhodochrosite-friedelite veins).

We believe that in the case of gasparite-(La) from the Wanni glacier, the source of arsenic was an As-rich hydrothermal fluid, as in the case of gasparite-(Ce) (Graeser and Schwander 1987) from the same area. More challenging to explain is the source of lanthanum. The host mineral could be the main source of REE, as was shown in the case of synchysite-(Ce) (Graeser and Schwander 1987), monazite-(Ce) (Ondrejka et al. 2007), and cervandonite-(Ce) (Guastoni et al. 2013). High P content in gasparite-(La) from the Wanni glacier indicates that monazite could be the host mineral. However, additional process of REE redistribution was needed, as (1) crystal of gasparite-(La) had La/Ce zoning and (2) (Ce)- and (Y)-dominant species were the rule in this region, supported by Ce/Y >> La in whole-rock samples (Hofmann and Knill 1996). Another possible explanation to La-enrichment is the partial oxidation of Ce^{3+} to insoluble Ce^{4+} during fluid transportation and subsequent LREE (La, Nd, Sm) enrichment. This mechanism is well recorded in uranyl minerals (e.g., Meisser et al. 2010).

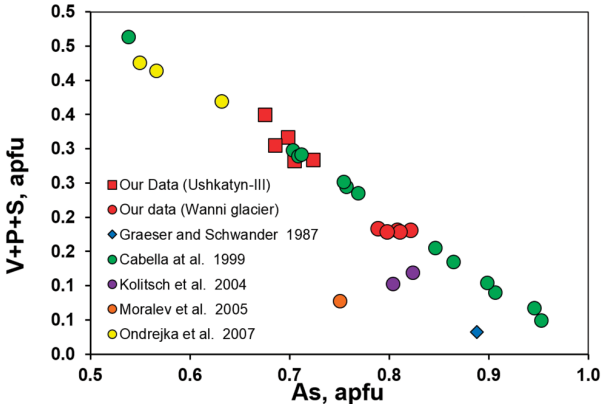

FIGURE 7. As vs. V+P+S substitution. (Color online.)

Thus, gasparite-(La) from the Wanni glacier was formed as a metasomatic mineral in the process of alteration of primary REE minerals by As-rich hydrothermal fluid and the ensuing La/Ce separation.

The Ushkatyn-III deposit is considered as an object of hydrothermal-sedimentary genesis, transformed by processes of low-grade regional metamorphism (Mitryaeva 1979; Skripchenko 1980; Rozhnov 1982; Brusnitsyn et al. 2018).

Gasparite-(La) from the Ushkatyn-III deposit was found in microveins in hausmannite ores. It was found in association with friedelite, jacobsite, pennantite, manganhumite series minerals, sarkinite, tilasite, and retzian-(La) and embedded into calcite-rhodochrosite veinlets. Similar veinlets in other rocks have a different composition. Calcite and quartz were found in microveins in the enclosing limestone. Calcite, kutnohorite, rhodonite, axinite-(Mn), friedelite, hematite, jacobsite, and barite were found in microveins in braunite ores. A regular change in the composition indicates the segregation mechanism of the genesis of such microveins. They were formed by local redeposition of a substance from the rocks in which they developed into thin cracks. These processes probably occurred during the period of

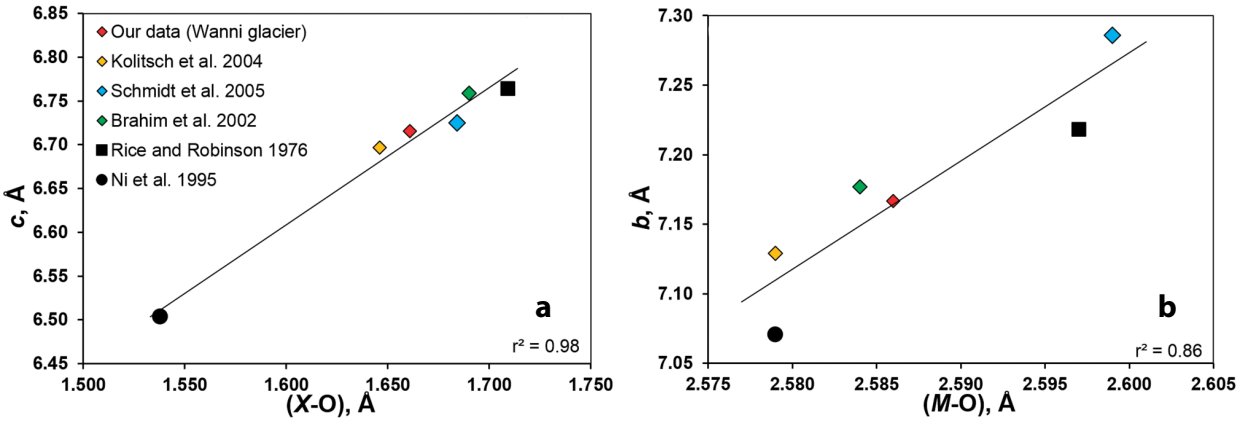

FIGURE 8. Unit-cell parameters of $M(XO_4)$ compounds (M = La, Ce; X = As, P, V): (**a**) c vs. (X-O) and (**b**) b vs. (M-O). (Color online.)

tectonic deformation of the region during Late Paleozoic time.

We believe that As and REE were accumulated syngenetically with manganese sediments in the Ushkatyn-III deposit. Most likely, the initial manganese oxides absorbed these elements, as it happens in modern oceans, where the absorption of REE to manganese oxides occurs much more intensively than many other precipitation minerals (Dubinin 2006).

The occurrence of As-minerals in the Ushkatyn-III deposit is connected to the manganese ores only and has not been found in the host rocks or tectonic deformation zones. Manganese rocks of different genesis are often enriched in arsenic, and more than half of all discovered Mn-arsenates were found in the famous Mn deposits (Frondel and Baum 1974; Abrecht 1990; Brugger and Giere 1999; Cabella et al. 1999; Holtstam and Langhof 1999; Lundström 1999; Brugger and Meisser 2006). Therefore, As and REE infiltration into ore layers from any external source is unlikely in this case.

Apparently, REE and As accumulated in the initial ore-bearing sediments as a component of Mn minerals. In the process of metamorphism and tectonic deformation, these elements were mobilized by pore solutions and re-deposited into secant ore veins. A similar mechanism for the genesis of REE-bearing arsenates is also assumed for metamorphosed Fe-Mn deposits in other regions (Cabella et al. 1999; Kolitsch et al. 2004).

TABLE 6. Selected bond lengths (Å) and the distortion of M-polyhedra for gasparite-(La) from the Wanni glacier and structurally related $M(XO_4)$ compounds (M = La, Ce; X = As, P, V)

Bond	Length					
	Gasparite-(La)	Gasparite-(Ce)	La(AsO_4)	Ce(AsO_4)	La(VO_4)	La(PO_4)
M–O1^{iii}	2.554 (2)	2.486(5)	2.571(3)	2.939(8)	2.521(4)	2.479(3)
M–O1^{iv}	2.481 (2)	2.527(5)	2.489(3)	2.636(9)	2.497(3)	2.554(3)
M–O2^{v}	2.479 (2)	2.902(5)	2.498(4)	2.460(7)	2.656(3)	2.783(3)
M–O2^{ii}	2.559 (2)	2.544(4)	2.560(4)	2.619(8)	2.568(3)	2.589(3)
M–O3^{ii}	2.901 (2)	2.632(5)	2.655(3)	2.472(8)	2.528(4)	2.615(3)
M–O3^{vi}	2.562 (2)	2.620(6)	2.577(3)	2.551(7)	2.677(4)	2.503(3)
M–O3	2.6440 (19)	2.457(5)	2.912(4)	2.562(7)	2.887(4)	2.672(3)
M–O4^{iii}	2.624 (2)	2.488(5)	2.644(4)	2.476(7)	2.533(4)	2.466(3)
M–O4^{vii}	2.472 (2)	2.555(4)	2.486(3)	2.543(7)	2.502(4)	2.548(3)
(M-O)	*2.586*	*2.579*	*2.599*	*2.584*	*2.597*	*2.579*
ΔM	*0.035*	*0.036*	*0.035*	*0.038*	*0.037*	*0.030*
X–O1	1.650 (2)	1.647(5)	1.670(4)	1.682(8)	1.724(4)	1.523(3)
X–O2	1.660 (2)	1.664(5)	1.680(4)	1.699(7)	1.720(4)	1.553(3)
X–O3	1.669 (2)	1.659(5)	1.695(4)	1.692(7)	1.699(4)	1.541(3)
X–O4	1.6656 (19)	1.615(5)	1.691(3)	1.686(8)	1.693(4)	1.537(3)
(X-O)	*1.661*	*1.646*	*1.684*	*1.690*	*1.709*	*1.538*
Reference	This study	Kolitsch et al. 2004	Schmidt et al. 2005	Brahim et al. 2002	Rice and Robinson 1976	Ni et al. 1995

Gasparite-(La) from the Ushkatyn-III deposit is characterized by relatively small amount of other REE (Ce+Nd+Pr < 0.3 apfu) compared to other gasparite-(Ce) (Fig. 6), and has a nearly constant La/Ce ratio. Its occurrence with retzian-(La) (Fig. 2) may indicate specific conditions of mineral formation in which rocks were depleted by cerium.

Lanthanum and cerium have very close chemical properties, but the average content of lanthanum in the Earth's crust is almost two times lower than cerium: 30 and 58 ppm, respectively (Li and Schoonmaker 2003). Gasparite-(La) and retzian-(La) formation require separating lanthanum from cerium. This could be done in two stages: (1) during the accumulation of manganese sediment or (2) later during lithification.

In favor of the first option is the fact that accumulations of manganese oxides of hydrothermal genesis are characterized by cerium deficiency relative to the remaining REE. In the REE spectra of such rocks, a negative cerium anomaly is usually well expressed (Dubinin 2006; Bau et al. 2014). In other words, La/Ce is higher in them than in "normal" marine sediments, which determines the possibility of the formation of lanthanum minerals. If this assumption is correct, then lanthanum minerals, including gasparite-(La) and retzian-(La), should be considered as indicators of the hydrothermal-sedimentary genesis of manganese ores. However, this issue requires further study.

According to the second option, the separation of lanthanum and cerium occurred at the post-sedimentation stage of the development of the deposit. The very low Ce content of both gasparite-(La) and retzian-(La) (less than 12 and 9 wt%, respectively) could be explained by formation from a strongly Ce-depleted source due to oxidation of Ce^{3+} and subsequent formation of insoluble cerianite-(Ce) as shown in the case of wakefieldite-(La) (Witzke et al. 2008). Cerianite-(Ce) was observed in several cases in the same samples from the Ushkatyn-III deposit where La arsenates were found. According to experimental data (Ohta and Kawabe 2001), the oxidation of cerium with manganese oxides proceeds according to the reaction:

$$2Ce^{3+} + MnO_2 + 2H_2O = 2CeO_2 + Mn^{2+} + 4H^+.$$

The reaction will shift to the right by a weak alkaline mineral formation medium, typical for carbonate associations. As a result, cerianite-(Ce) can coexist with Mn^{2+} minerals (rhodochrosite, tephroite, friedelite, etc.). However, it is possible only in the absence of organic matter. Otherwise, there will be a dissolution of cerianite-(Ce) with the restoration of cerium by the reaction (Dubinin 2006):

$$CH_2O + 5H_2O + 11CO_2 + 4CeO_2 \rightarrow 4Ce^{3+} + 12HCO_3^-.$$

Accordingly, the formation of cerianite-(Ce) and, as a consequence, the formation of La-rich (Ce-depleted) minerals are controlled by the local distribution of Mn, REE, and organic matter.

Both scenarios considered (cerium deficiency in initial sediments and cerium concentration in cerianite-(Ce) at post-sedimentary stages) do not contradict each other. Most likely, each of them contributed to the formation of gasparite-(La) and other La-rich minerals in manganese ores of the Ushkatyn-III deposit.

Thus, gasparite-(La) from the Ushkatyn-III deposit was formed in primary ores and was not influenced by metasomatic processes. We believe that it is precisely the features of the chemical composition of the initial Mn-Fe ores that predetermined the possibility of the formation of lanthanum minerals in the Ushkatyn-III deposit.

Implications

Gasparite-(La) from Mn ores of the Ushkatyn-III deposit and metamorphic rocks of the Wanni glacier have different geological settings and different formation conditions. Thus, an occurrence of gasparite-(La) in rocks and its chemical composition could be used as a tool for geological reconstruction of their host rock formation.

In the case of gasparite-(La) from the Ushkatyn-III deposit, both REE and As were sourced from the host Mn ores. In all analyzed grains, the As/V/P and La/Ce ratios are nearly constant, while As > V > P and La > Ce. Constant lanthanum predominance in analyzed gasparite grains indicates specific conditions of Mn ore formation: Ce depletion or La enrichment and no metasomatic process. Besides that, gasparite from Mn ores is characterized by low P and high V content (our data; Cabella et al. 1999). Modern metalliferous sediment is mainly composed of Fe- and Mn-oxy/hydroxides and smectite minerals (e.g., Vereshchagin et al. 2019), which are carriers of V and REE (Gurvich 2006). Ferromanganese ores are sources of several REE-dominant vanadates (Moriyama et al. 2011; Witzke et al. 2008). Thus, the content of V originated from primary Fe-,Mn-sediments could be used as an indicator of gasparite origin.

Gasparite-(La) from the Wanni glacier has different chemical features. Although its As/V/P ratio is also nearly constant, in its As > P > V. High P content is a typical feature of gasparite from metasomatic rocks (Graeser and Schwander 1987; Ondrejka et al. 2007). In addition, it has variable La/Ce ratios, which is typical for gasparite from metasomatic rocks, probably due to La/Ce separation during recrystallization.

Funding

The work was carried out using the analytical capabilities of the Resource Centers of St. Petersburg State University "X-ray Diffraction Centre," "Microscopy and Microanalysis," "Innovative Technologies of Composite Nanomaterials", and "Geomodel".

Acknowledgments

We are grateful to Mischa Crumbach (Visp, Switzerland) for providing the picture of a gasparite-(La) crystal from the Wanni glacier. We express our gratitude to A.Yu. Burkovski, Chairman of the Board of Zhayremsky GOK JSC and A.V. Volkov, Chief Geologist of Zhairemsky GOK JSC for assistance in the implementation of fieldwork. Technical assistance in sample preparation by D.A. Popov is highly appreciated. The authors gratefully acknowledge Evgeny V. Galuskin and two anonymous reviewers for their helpful comments.

References cited

Abrecht, J. (1990) An As-rich manganiferous mineral assemblage from the Ködnitz Valley (Eastern Alps, Austria): Geology, mineralogy, genetic considerations, and implications for metamorphic Mn deposits. Neues Jahrbuch für Mineralogie, 363–375.

Anthony, J.W., Bideaux, R.A., Bladh, K.W., and Nichols, M.C. (2000) Handbook of Mineralogy. Mineralogical Society of America, Chantilly, Virginia.

Appiani, R., Majrani, M., and Sacchi, M. (2017) Gioielli delle Alpi italiane. Ediz. illustrata. 400 p.

Armbruster, T., Buhler, C., Graeser, S., Stalder, H.A., and Amthauer, G. (1988) Cervandonite-(Ce), $(Ce,Nd,La)(Fe^{3+},Fe^{2+},Ti^{4+},Al)_3SiAs(Si,As)O_{13}$, a new Alpine fissure mineral. Schweizerische Mineralogische und Petrographische Mitteilungen, 68, 125–132.

Ashley, P.M. (1989) Geochemistry and mineralogy of tephroite-bearing rocks from the Hoskins manganese mine, New South Wales, Australia. Neues Jahrbuch für Mineralogie, Abhandlungen, 161, 85–111.

Barros, G., Santos, C.C., Ayala, A.P., Guedes, I., Boatner, L.A., and Loong, C.-K. (2009) Raman investigations of rare-earth arsenate single crystals. Journal of Raman Spectroscopy, 41(6), 694–697.

Bau, M., Scmidt, K., Koschinsky, A., Hein, J., Kuhn, T., and Usui, A. (2014) Discriminating between different genetic types of marine ferro-manganese crusts and nodules on rare earth elements and yttrium. Chemical Geology, 381, 1–9.

Bayliss, P., and Levinson, A.A. (1988) A system of nomenclature for rare-earth mineral species: Revision and extension. American Mineralogist, 73, 422–423.

Beall, G.W., Boatner, L.A., Mullica, D.F., and Milligan, W.O. (1981) The structure of cerium ortho-phosphate, a synthetic analog of monazite. Journal of Inorganic and Nuclear Chemistry, 43, 101–105.

Bedlivy, D., and Mereiter, K. (1982) Structure of α-$BiAsO_4$ (rooseveltite). Acta Crystallographica, B38, 1559–1561.

Bergomi, M.A., Dal Piaz, G.V., Malusà, M. G., Monopoli, B., and Tunesi, A. (2017) The Grand St Bernard-Briançonnais nappe system and the Paleozoic inheritance of the Western Alps unraveled by zircon U-Pb dating. Tectonics, 36, 2950–2972.

Botto, I.L., and Baran, E.J. (1982) Characterization of the monoclinic rare earth orthoarsenates. Journal of the Less Common Metals, 83, 255–261.

Brahim, A. Mongi, F.M., and Amor, H. (2002) Cerium arsenate, $CeAsO_4$. Acta Crystallographica, E58, 98–99.

Breiter, K., Čopjaková, R., and Škoda, R. (2009) The involvement of F, CO_2, and As in the alteration of Zr-Th-REE-bearing accessory minerals in the Hora Svaté Kateøiny A-type granite, Czech Republic. Canadian Mineralogist, 47, 1375–1398.

Britvin, S.N., Dolivo-Dobrovolsky, D.V., and Krzhizhanovskaya, M.G. (2017) Software for processing the X-ray powder diffraction data obtained from the curved image plate detector of Rigaku RAXIS Rapid II diffractometer. Proceedings of the Russian Mineralogical Society, 146, 3, 104–107.

Brugger, J., and Giere, R. (1999) As, Sb, Be and Ce enrichment in minerals from a metamorphosed Fe–Mn deposits, Val Ferrera, Eastern Swiss Alps. Canadian Mineralogist, 37, 37–52.

Brugger, J., and Meisser, N. (2006) Manganese-rich assemblages in the Barrhorn unit, Turtmanntal, central Alps, Switzerland. Canadian Mineralogist, 44, 229–248.

Brusnitsyn, A.I., Perova, E.N., Vereshchagin, O.S., Letnikova, E.F., Shkolnik, S.I., and Ivanov, A.V. (2017) Stratiform lead-zinc and iron-manganese ores of the Zhayremsky ore cluster (Central Kazakhstan): conditions of occurrence, composition, genesis. Metallogeny of ancient and modern oceans. Differentiation and reasons for the diversity of ore deposits. Miass: IMIN UB RAS, p. 90–94 (in Russian).

Brusnitsyn, A.I., Perova, E.N., Vereshchagin, O.S., Britvin, S.N., Platonova, N.V., and Shilovskikh, V.V. (2018) Genetic mineralogy of manganese ores of Ushkatyn-III deposit, Central Kazakhsan. Metallogeny of ancient and modern oceans. Volcanism and ore formation. Miass: IMIN UB RAS, p. 67–70 (in Russian).

Buzmakov, E.I., Shibrik, V.I., Rozhnov, A.A., Sereda, V.Ya., and Radchenko, N.M. (1975) Stratiform iron-manganese and polymetallic deposits of the Ushkatynsky ore field (Central Kazakhstan). Geology of Ore Deposits, 1, 32–46 (in Russian).

Cabella, R., Lucchetti, G., and Marescotti, P. (1999) Occurrence of *LREE*- and Y-arsenates from a Fe-Mn deposit, Ligurian Briançonnais Domain, Maritime Alps, Italy. Canadian Mineralogist, 37, 961–972.

Campbell, K.M., and Nordstrom, D.K. (2014) Arsenic speciation and sorption in natural environments. Reviews in Mineralogy and Geochemistry, 79, 185–216.
Clavier, N., Podor, R., and Dacheux, N. (2011) Crystal chemistry of the monazite structure. Journal of the European Ceramic Society, 31, 941–976.
Cuchet, S., van der Burgt, A., and Meisser, N. (2005) Chummibort, eine neue Fundstelle für Arsenmineralien im Binntal. Schweizer Strahler, 2, 19–29.
Cuchet, S., Crumbach, M., Van der Burgt, A., Vanini, F., Loranth, C., Mestrom, P., Antonysen, E., Meisser, N., and Roth, P. (2019) Mineralogische Topografie der Schweiz und angrenzender Regionen 1. Teil–Binntal (CH)–Veglia (1)–Devero (1), Schweizer Strahler, 1/2019, S. 2-17.
Deliens, M., and Piret, P. (1986) Kusuite becomes plombean wakefieldite (Ce). Bulletin de Mineralogie, 109(3), 305.
Demartin, F., Gramaccioli, C.M., and Pilati, T. (1994) Paraniite-(Y), a new tungstate arsenate mineral from Alpine fissures. Schweizerische Mineralogische und Petrographische Mitteilungen, 74, 155–160.
Dolomanov, O.V., Bourhis, L.J., Gildea, R.J., Howard, J.A., and Puschmann, H. (2009) OLEX2: a complete structure solution, refinement and analysis program. Journal of Applied Crystallography, 42, 339–341.
Dubinin, A.V. (2006) Geochemistry of Rare Earth Elements in the Ocean. Moscow, Nauka Publ. 359 p. (in Russian).
Dunn, P.J., Peacor, D.R., and Simmons, W.B. (1984) Retzian-(La), a new mineral from Sterling Hill, Sussex County, New Jersey. Mineralogical Magazine, 48, 533–535.
Feigelson, R.S. (1964) Synthesis and single-crystal growth of rare-earth orthophosphates. Journal of the American Ceramic Society, 47, 257–258.
Foord, E.E., Hlava, P.F., Fitzpatrick, J.J., Erd, R.C., and Hinton, R.W. (1991) Maxwellite and squawcreekite, two new minerals from the Black Range tin district, Catron County, New Mexico. Neues Jahrbuch fur Mineralogie, Monatshefte, 363–384.
Foord, E.E., Hughes, J.M., Cureton, F., Maxwell, C.H., Flaster, A.U., Sommer, A.J., and Hlava, P.F. (1999) Esperanzaite, $NaCa_2Al_2(As^{5+}O_4)_2F_4(OH)\cdot 2H_2O$, a new mineral species from the La Esperanza Mine, Mexico: Descriptive mineralogy and atomic arrangement. Canadian Mineralogist, 37, 67–72.
Förster, H.-J., Ondrejka, M., and Uher, P. (2011) Mineralogical responses to subsolidus alteration of granitic rocks by oxidizing As-bearing fluids: REE arsenates and As-rich silicates from the Zinnwald granite, eastern Erzgebirge, Germany. Canadian Mineralogist, 49, 913–930.
Frondel, C., and Baum, J. (1974) Structure and mineralogy of the Franklin zinc-iron-manganese deposit, New Jersey. Economic Geology, 69, 157–180.
Gatta, D.G., Rotiroti, N., Cámara, F., and Meven, M. (2018) On the labyrinthine world of arsenites: a single-crystal neutron and X-ray diffraction study of cafarsite. Physics and Chemistry of Minerals, 45, 9, 819–829.
Ghouse, K.M. (1968) Refinement of crystal structure of heat-treated monazite crystal. Indian Journal of Pure and Applied Physics, 6, 265–268.
Graeser, S. (1966) Asbecasit und Cafarsit, zwei neueMineralien aus dem Binnatal (Kt. Wallis). Schweizerische Mineralogische und Petrographische Mitteilungen, 46, 367–375.
Graeser, S., and Roggiani, A.G. (1976) Occurrence and genesis of rare arsenate and phosphate minerals around Pizzo Cervandone, Italy/Switzerland. Rendicontri della Societa Italiana di Mineralogia e Petrologia, 32, 279–288.
Graeser, S., and Schwander, H. (1987) Gasparite-(Ce) and monazite-(Nd): two new minerals to the monazite group from the Alps. Schweizerische Mineralogische und Petrographische Mitteilungen, 67, 101–113.
Graeser, S., Schwander, H., Demartin, F., Gramaccioli, C.M., Pilati, T., and Reusser, E. (1994) Fetiasite $(Fe^{2+}, Fe^{3+}, Ti)_3O_2[As_2O_5]$, a new arsenite mineral: its description and structure determination. American Mineralogist, 79, 996–1002.
Guastoni, A., Pezzota, F., and Vignola, P. (2006) Characterization and genetic inferences of arsenates, sulfates and vanadates of Fe, Cu, Pb, Zn from Mount Cervadone (Western Alps, Italy). Periodico di Mineralogia, 75, 141–150.
Guastoni, A., Nestola, F., Gentile, P., Zorzi, F., Alvaro, M., Lanza, A., Peruzzo, L., Schiazza, M., and Casati, N.M. (2013) Deveroite-(Ce): a new REE-oxalate from Mount Cervandone, Devero Valley, Western-Central Alps, Italy. Mineralogical Magazine, 77, 3019–3026.
Gurvich, E.G. (2006) Metalliferous sediments of the world ocean. Fundamental Theory of Deep-sea Hydrothermal Sedimentation, 416 p. Springer. DOI: 10.1007/3-540-30969-1
Hettmann, K., Kreissig, K., Rehkämper, M., Wenzel, T., Mertz-Kraus, R., and Markl, G. (2014) Thallium geochemistry in the metamorphic Lengenbach sulfide deposit, Switzerland: Thallium-isotope fractionation in a sulfide melt. American Mineralogist, 99, 793–803.
Hofmann, B., and Knill, M.D. (1996) Geochemistry and genesis of the Lengenbach Pb-Zn-As-Tl-Ba-mineralisation, Binn Valley, Switzerland. Mineralium Deposita, 31, 319–339.
Holtstam, D., and Langhof, J. (Eds.) (1999) Langban, the Mines, their Minerals, History and Explorers, 215 p. Raster Forlag, Stockholm.
Kang, D.-H., and Schleid, T. (2005) Einkristalle von $La[AsO_4]$ im Monazit- und $Sm[AsO_4]$ im Xenotim-Typ. Zeitschrift für Anorganische und Allgemeine Chemie, 631, 10, 1799–1802.
Kayupova, M.M. (1974) Mineralogy of iron and manganese ores of the Western Atasu (Central Kazakhstan). Alma-Ata, Nauka, 232 p. (in Russian).
Klemm, L., Pettke, T., Graeser, S., Mullis, J., and Kouzmanov, K. (2004) Fluid mixing as the cause of sulphide precipitation at Albrunpass, Binn Valley, Central Alps. Schweizerische Mineralogische und Petrographische Mitteilungen, 84, 189–212.
Kolitsch, U., and Holtstam, A. (2004) Crystal chemistry of $REEXO_4$ compounds (X = P, As, V). II. Review of $REEXO_4$ compounds and their stability fields. European Journal of Mineralogy, 16, 117–126.
Kolitsch, U., Holtstam, D., and Gatedal, K. (2004) Crystal chemistry of $REEXO_4$ compounds (X = P, As, V). I. Paragenesis and crystal structure of phosphatian gasparite-(Ce) from the Kesebol Mn-Fe-Cu deposit, Västra Götaland, Sweden. European Journal of Mineralogy, 16, 111–116.
Krzemnicki, M. (1992) As-Bi-Mineralisationen in der Monte-Leone-Decke im Mättital (Binntal-Region). Thesis, Universität Basel, Switzerland, 122 p.
——— (1997) Mineralogical investigations on hydrothermal As- and REE-bearing minerals within the gneisses of the Monte-Leone nappe (Binntal region, Switzerland). Dissertation, Universität Basel, Switzerland, 86 p.
Krzemnicki, M.S., and Reusser, E. (1998) Graeserite, $Fe^{3+}_4Ti_3As^{3+}O_{13}(OH)$ a new mineral species of the derbylite group from from the Mount Leone Nappe, Binntal Region, Western Alps, Switzerland. Canadian Mineralogist, 36, 1083–1088.
Le Berre, J.-F., Gauvin, R., and Demopoulos, G. P. (2007) Synthesis, structure, and stability of gallium arsenate dihydrate, indium arsenate dihydrate, and lanthanum arsenate. Industrial and Engineering Chemistry Research, 46, 7875–7882.
Li, Y.-H., and Schoonmaker, J.E. (2003) Chemical composition and mineralogy of marine sediments. Treatise on Geochemistry. Sediments, Diagenesis, and Sedimentary Rocks, 7, 1–35.
Lundström, I. (1999) General geology of the Bergslagen ore region. In D. Holtstam and J. Langhof, Eds., Långban. The Mines, Their Minerals, Geology and Explorers, p. 19–27. Christian Weise Verlag.
Majzlan, J., Drahota, P., and Filippi, M. (2014) Parageneses and crystal chemistry of arsenic minerals. Reviews in Mineralogy and Geochemistry, 79, 17–184.
Mancini, S. (2000) Le mineralizzazioni a manganese delle Alpi Apuane. Tesi di Laurea, University of Pisa.
Maxelon, M., and Mancktelow, N.S. (2005) Three-dimensional geometry and tectonostratigraphy of the Pennine zone, Central Alps, Switzerland and Northern Italy. Earth Science Reviews, 71, 171–227.
Maynard, J.B. (2003) Manganiferous sediments, rocks and ores. Treatise on Geochemistry. Sediments, Diagenesis, and Sedimentary Rocks, 7, 289–308.
Meisser, N., Brugger, J., Ansermet, S., Thelin, P., and Bussy, F. (2010) Francoisite-(Ce), a new mineral species from La Creusaz uranium deposit (Valais, Switzerland) and from Radium Ridge (Flinders Ranges, South Australia): Description and genesis. American Mineralogist, 95, 1527–1532.
Mills, S., Kartashov, P.M., Kampf, A.R., and Raudsepp, M. (2010) Arsenoflorencite-(La), a new mineral from the Komi Republic, Russian Federation: description and crystal structure. European Journal of Mineralogy, 22, 613–621.
Mitryaeva, N.M. (1979) Mineralogy of barite-zinc-lead ores of Atasuisky district. Alma-Ata, Nauka, 219 p. (in Russian).
Modresky, P.J. (1983) Agardite-(La), a chemically complex rare-earth arsenate from the gallinas district, Lincoln Co., New Mexico. In J.W. Anthony, Ed., Oxidation Mineralogy of Base Metal Deposits, Fifth Joint Mineralogical Society of America—Friends of Mineralogy Symposium.
Mooney, R.C.L. (1948) Crystal structures of a series of rare earth phosphates. The Journal of Chemical Physics, 16, 1003.
Moralev, G.V., Borisov, A.V., Surenkov, S.V., Nagaeva, S.P., Tarbaev, M.B., Kuznetsov, S.K., Onishchenko, S.A., Efanova, L.I., and Soboleva, A.A. (2005) Distribution and modes of occurrence of REE at the Chudnoe and Nesterovskoe occurrences of Au–Pd–REE ore mineralization in the Maldynyrd Range, Nether-Polar Urals. Geochemistry International, 43, 11, 1078–1097.
Moriyama, T., Miyawaki, R., Yokoyama, K., Matsubara, S., Hirano, H., Murakami, H., and Watanabe, Y. (2011) Wakefieldite-(Nd), a new neodymium vanadate mineral in the Arase stratiform ferromanganese deposit, Kochi Prefecture, Japan. Resource Geology, 61, 101–110.
Mullica, D.F., Milligan, W.O., Grossie, D.A., Beall, G.W., and Boatner, L.A. (1984) Ninefold coordination in $LaPO_4$—pentagonal interpenetrating tetrahedral polyhedron. Inorganica Chimica Acta, 95, 231–236.
Mullica, D.F., Grossie, D.A., and Boatner, L.A. (1985) Structural refinements of praseodymium and neodymium ortho-phosphate. Journal of Solid State Chemistry, 58, 71–77.
Ni, Y., Hughes, J.M., and Mariano, A.N. (1995) Crystal chemistry of the monazite and xenotime structures. American Mineralogist, 80, 21–26.
Ohta A., Kawabe I. (2001) REE(III) adsorption onto Mn dioxide (δ-MnO_2) and Fe oxyhydroxide: Ce(III) oxidation by δ-MnO_2. Geochimica et Cosmochimica Acta, 65, 695–703.
Ondrejka, M., Uher, P., Pršek, J., and Ozdín, D. (2007) Arsenian monazite-(Ce) and xenotime-(Y), REE arsenates and carbonates from the Tisovec-Rejkovo rhyolite, Western Carpathians, Slovakia: Composition and substitutions in the $(REE,Y)XO_4$ system (X = P, As, Si, Nb, S). Lithos, 95, 116–129.
Pepin, G.J., and Vance, E.R. (1981) Crystal data for rare earth orthophosphates of the monazite structure-type. Journal of Inorganic and Nuclear Chemistry,

43(II), 2807–2809.
Raison, P.E., Jardin, R., Bouexiere, D., Konings, R.J.M., Geisler, T., Pavel, C.C., Rebizant, J., and Popa, K. (2008) Structural investigation of the synthetic CaAn $(PO_4)_2$ (An = Th and Np) cheralite-like phosphates. Physics and Chemistry of Minerals, 35, 603–609.
Roth, P., and Meisser, N. (2013) Die seltenen Mineralien der Büdner Mangan-vorkommen. Schweizer Strahler, 47, 3, 8–21.
Rozhnov, A.A. (1982) Comparative characteristics of manganese deposits of Atasuisky and Nikopol-Chiatura types. In: Geology and geochemistry of manganese, Moscow, Nauka, 116–121 (in Russian).
Schmidt, M., Müller, U., Cardoso-Gil, R., Milke, E., and Binnewies, M. (2005) Zum Chemischen Transport und zur Kristallstruktur von Seltenerdarsenaten(V). Zeitschrift für anorganische und allgemeine Chemie, 631, 1154–1162.
Schwarz, H. (1963) The phosphates, arsenates, and vanadates of the rare earths. Zeitschrift für anorganische und allgemeine Chemie, 323, 44–56.
Schwartz, A.J., Kumar, M., and Adams, B.L. (2009) Electron Backscatter Diffraction in Materials Science. Springer.
Sheldrick, G.M. (2015) Crystal structure refinement with SHELXL. Acta Crystallographica, C71, 3–8.
Skripchenko, N.S. (1980) Hydrothermal-sedimentary polymetallic ores of calc-slate formations. Moscow, Nedra, 215 p. (in Russian).
——— (1989) Forecasting deposits of non-ferrous metals in sedimentary rocks. Irkutsk, Nedra, 207 p (in Russian).
Solecka, U., Bajda, T., Topolska, J., Zelek-Pogudz, S., and Manecki, M. (2018) Raman and Fourier transform infrared spectroscopic study of pyromorphite-vanadinite solid solutions. Spectrochimica Acta Part A: Molecular and Biomolecular Spectroscopy, 190, 96–103.
Song, H., Liub, J., and Cheng, H. (2018) Structural and spectroscopic study of arsenate and vanadate incorporation into apatite group: Implications for semi-quantitative estimation of As and V contents in apatite. Spectrochimica Acta Part A: Molecular and Biomolecular Spectroscopy, 188, 488–494.
Steck, A. (1987) Le massif du Simplon. Reflexions sur la cinematique des nappes de gneiss. Schweizerische Mineralogische und Petrographische Mitteilungen, 67, 27–45.
Streckeisen, A., Wenk, E., and Frey, M. (1974) On steep isogradic surfaces in the Simplon area. Contributions to Mineralogy and Petrology, 47, 8l–95.
Vereshchagin, O.S., Perova, E.N., Brusnitsyn, A.I., Ershova, V.B., Khudoley, A.K., Shilovskikh, V.V., and Molchanova, E.V. (2019) Ferro-manganese nodules from the Kara Sea: Mineralogy, geochemistry and genesis. Ore Geology Reviews, 106, 192–204.
Witzke, T., Kolitsch, U., Warnsloh, J.M., and Göske, J. (2008) Wakefieldite-(La), a new mineral species from the Glücksstern Mine, Friedrichroda, Thuringia, Germany. European Journal of Mineralogy, 20, 1135–1139.
Wu, Y., Kukkadapu, R.K., Livi, K.J.T., Xu, W., Li, W., and Sparks, D.L. (2018) Iron and arsenic speciation during As(III) oxidation by manganese oxides in the presence of Fe(II): molecular-level characterization using XAFS, Mössbauer, and TEM analysis. ACS Earth and Space Chemistry, 2, 256–268.
Yang, H., Downs, R.T., Jenkins, R.A., and Evans, S.H. (2018) Segerstromite, $Ca_3(As^{5+}O_4)_2[As^{3+}(OH)_3]_2$, the first mineral containing $As^{3+}(OH)_3$, the arsenite molecule, from the Cobriza mine in the Atacama Region, Chile. American Mineralogist, 103, 1497–1501.

Manuscript received March 4, 2019
Manuscript accepted June 15, 2019
Manuscript handled by Daniel Hummer

Endnote:

[1]Deposit item AM-19-107028, CIF and Supplemental Material. Deposit items are free to all readers and found on the MSA website, via the specific issue's Table of Contents (go to http://www.minsocam.org/MSA/AmMin/TOC/2019/Oct2019_data/Oct2019_data.html).